Image Enhancement and Segmentation Techniques for Detection of Knee Joint Diseases: A Survey

Tanzila Saba, Amjad Rehman *, Zahid Mehmood, Hoshang Kolivand and Muhammad Sharif

[1]College of Computer and Information Sciences Prince Sultan University Riyadh 11586 Saudi Arabia

[2]College of Computer and Information Systems Al-Yamamah University Riyadh 11512 Saudi Arabia

[3]Department of Software Engineering, University of Engineering and Technology Taxila-47050, Pakistan

[4]Department of Computer Science, Liverpool John Moores University, Liverpool, UK, L3 3AF

[5]Department of Computer Science, COMSAT University Islamabad Wah Campus Pakistan

Abstract

Knee bone diseases are rare but might be highly destructive. Magnetic resonance imaging (MRI) is the main approach to identify knee cancer and its treatment. Normally, the knee cancers are pointed out with the help of different MRI analysis techniques and latter image analysis strategies understand these images. Computer-based medical image analysis is getting researcher's interest due to its advantages of speed and accuracy as compared to traditional techniques. The focus of current research is MRI-based medical image analysis for knee bone disease detection. Accordingly, several approaches for features extraction and segmentation for knee bone cancer are analyzed and compared on benchmark database. Finally, the current state of the art is investigated and future directions are proposed.

Keywords: Knee bone disease; knee image analysis; MRI; Knee image segmentation; Features mining.

1. Introduction

Computers are being used in a verity of fields and digital images have a great effect on modern society. The field of medicine is one of the areas that received the greatest impact from the computer. Medical images have turned into an imperative piece of therapeutic determination and treatment [1]. Medical images play a considerable part in medical applications since specialists are occupied with uncovering inward life structures. Several techniques are reported in the state of art depends on cross-sectional images such as computed tomography (CT), X-ray, MRI or some other tomographic modalities PET, SPECT, ultrasound etc. [2, 3]. Currently, medical image processing is a significant areas in the field of image processing that analyzes the problems and applications of medical images.

Various applications of medical image processing are Image segmentation, image record-keeping, and image-directed surgical treatments. Image segmentation is the most vital area of image processing as it extracts the region of interest by automatic or semi-automatic method [4, 5]. Numerous segmentation techniques have been utilized as a part of the restorative application to fragment the tissues and body organs and the results have been used wildly in surgeries and clinical applications[6, 7].

This research starts with an overview of magnetic resonance imaging techniques with their pros and cons. It follows by describing pre-processing tasks like images enhancement and feature extraction. Description of several segmentation methods has been explained and followed by post-processing techniques. Moreover, current paper is arranged into three main sections; section 2 highlights pre-processing techniques for MRI, section 3 presents MRI segmentation techniques and paper is concluded in section 4.

2. Magnetic Resonance Imaging (MRI)

Commonly used medical imaging techniques are X-ray, CT, ultrasound and MRI. X-ray is the oldest modality among all, and it has been in practice for over a century. This system utilizes Electromagnetic radiation with a short wavelength and intense vitality. The frequency of this radiation is between 10^6 and 10^{21} Hertz. The X-ray hit the organs and makes a negative image because the shadows are white regions and objects are gray. Nowadays, X-ray has been used widely for most of the body organs like joints, bones and chest cavity[8-10].

CT is the other medical imaging technique, in which X-ray is used to take images of the body parts. CT scanner machine moves beside the body and scans the desired organ. It makes several equivalent parts from each organ by passing X-ray beams through body. Every X-ray beat keeps going only a small amount of a moment and produces a portion of the organ or region of interest. For printing or future study the produced image slice are saved by computer. In this technology, hard tissues appear by white color and soft tissues appear by dark and graycolors[11-13]. CT arthrography image is shown in further down figure.

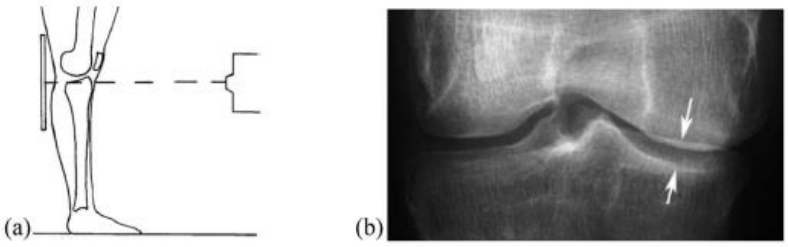

Figure 1: CT arthrography, Knee radiograph with horizontal beam [14]

MRI is relatively young medical imaging technique which depends on the physical phenomenon of nuclear magnetic resonance (NMR). It produces exceptionally high-quality 2D/3D images of human anatomic tissues by utilizing the hydrogen's interaction with a

strong external magnetic field and radio frequency. In the neuroimaging domain, MRI is superior to other imaging techniques, such as CT, ultrasound, and X-ray, and has already become the primary technique for neurological diagnosis and treatment [15, 16].

MRI is a medical imaging technique that becomes famous during this decade. This technique is still immature and under observation of several researchers. The history of MRI comes back to Felix Bloch and Edward Purcell who discovered the magnetic resonance phenomenon autonomously in 1946 and they got Nobel Prize in 1952. The first small sample tube presented by Paul Lauterbur, in 1973. Using phase and frequency encoding, and the Fourier Transform, Richard Ernst presented magnetic resonance imaging in 1975. It became the foundation of current MRI techniques. Whole body MRI presented by Raymond Damadian, in 1977[17, 18]. In 1980, Ernst's technique has been used by Edelstein and co-workers to perform established imaging of the body. This technique could be produced a single image in almost five minutes. In 1986, this achievement decreased to around five seconds. The first business model MR scanner was generated at Helsinki University Central Hospital, in June 1982. From this time many companies start to produce MR machines, such as PHILIPS Medical Systems, GE Medical Systems, TOSHIBA America Medical Systems (TAMS), HITACHI Medical, and SIEMENS Medical Solution[19, 20]. In 1993, new functional MRI produced and started a new research in this area. Clinics and hospitals bought around 1,300 MRI machine until 1988. More than 17,000 MRI machine is using in hospitals around the world and more than 2,500 scanners are installed each year[21].

In MRI imaging patient should be put in the machine during the operation. Magnetic field makes effects on hydrogen atoms of body organs and aligns them to the same or opposite direction with this field. A powerful radio signal is passed through the patient's body that excited the hydrogen atoms with the same frequency as the radio wave. Mean is that hydrogen atoms will be raised to a higher state of energy and start to resonate with the exciting wave. After turning off the radio signal the hydrogen atoms will back to original energy state. During the coming back to the previous energy, hydrogen atoms release the excited energy which they gained from radio signals[22, 23]. MRI machine detects released energy and converts it to readable data. The number of atoms, their characteristics, and tissues properties has an important effect on taking time for excited hydrogen atoms to come back to their original energy. This time is taken to generate one slice, thus for producing a number of parallel slices in MRI, it takes the number of slices multiply to time for one slice[24, 25].

The whole part of the body is included from water, which is around 70%. A water molecule is included hydrogen atoms. In MRI considered to this subject and it has been used to produce a novel imaging technique. One of the measurements for the magnet in MRI equipment is Tesla and the other popular measurement is Gauss. Each Tesla is equal to 10,000 Gauss. Tesla domain that is using in MRI is from 0.5 to 2.0 Tesla that is equal to 5,000 to 20,000 Gauss. Magnetic fields more than 2 Tesla cannot be used for medical imaging.

Against the CT-scan and X-ray which let us produce an image in one direction MRI machine obtain images in three planes which are the sagittal plane, the horizontal plane, and coronal plane[26]. These three imaging planes are shown in figure 2.

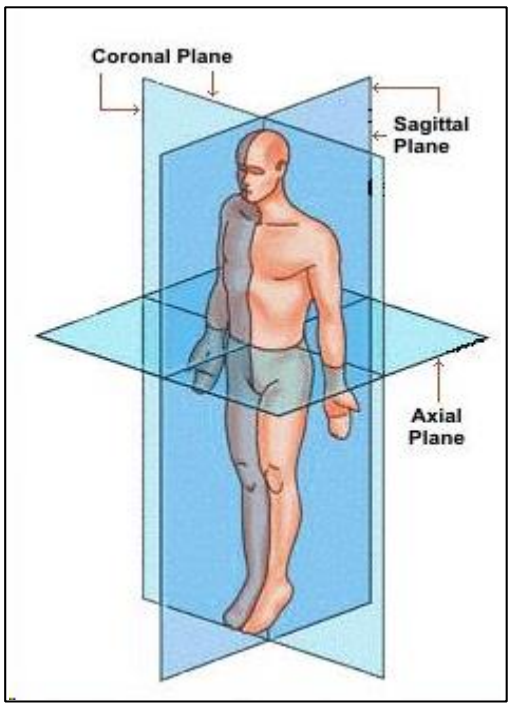

Figure 2: Three planes imaging in MRI techniques [26].

The MRI imaging is done around three axes which are:

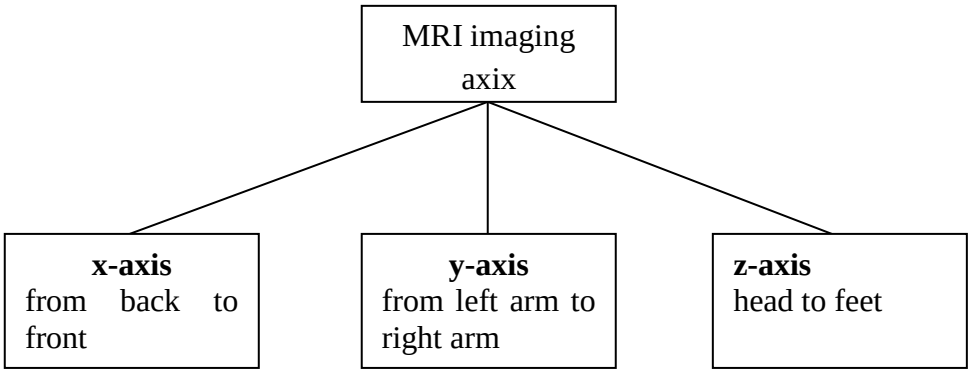

Figure 3: MRI imaging axis

Relaxation is one the important factor in MRI, which is the time period that the proton, which is, located in nuclei of atoms release the energy. This period is the time when excited nuclei come back from high energy to the low energy. T1 and T2 are biological parameters that control the relaxation factor[27-29]. These parameters define the ability to separate different

tissues from each other. The time constant of z-direction called T1 or spin-lattice relaxation time and the time constant of XY-plane called T2 or spin-spin relaxation time is relaxation process and time. These two parameters are related to tissue's physical interactions, which are around 2-3 seconds in pure water. T1 is considerably greater than T2 In biological materials. T1/T2 relaxation times have differences in different tissues, which lead to construct the image by the recording of these times. MRI imaging has produced three types of MR images, which are T1, T2, and Proton Density (PD)-weighted images. T1 relaxation time comparison of different tissues can produce T1-weighted images; T2 relaxation time comparison of different tissues could produce T2-weighted images and calculating the sum of protons per unit in each tissue produce PD-weighted images[30, 31].

An MRImachine include of six elements: magnet, shim coils, radio frequency (RF) coil, receiver coil, gradient coils, computer.

One of the drawbacks in MRI is intensity in homogeneity. Mean that in MRI imaging the intensity of same tissues does not have constant intensity over the image domain. In the other word, pixels in the same tissues some time have differences and pixels in the different tissues some time have similarities due to two main causes. The first one is the magnetic field with a static fault; the second one is the faulty RF coils and the variable magnetization ability between RF coils and patients[32, 33].

2.1 Pre-processing

This section presents pre-processing techniques that are performed prior to segmentation process. The result of this step improves the image for segmentation task and extract useful feature to apply in subsequent steps.

2.1.1 Image Enhancement

Image enhancement is image processing chore to increase appearance for human and to makes better contrast and visibility of features. It fundamentally improving image information for human viewers and generate a better image to input to further automatic image processing methods. Manipulate characteristics and features of an image to improve it for a special chore and the definite spectator is the basic objective of image enhancement. Some features and characteristics are improved during this task. Many image enhancements have been presented for each specific purpose, but they are divided into two main parts[34, 35]:

a. Spatial Domain Methods
b. Frequency Domain Methods

Applying some methods or formula is used to map images pixel in spatial domain method, but in frequency domain methods, Fourier transform is used to improve images. These operations are applied to adjust the image brightness, contrast or distribution of the gray

levels. Images pixels are changed according to the methods to achieve desired values to get improved image [25, 30, 36].

In image enhancement, we can declare T transformation to map values from image f into g. the parameter r and s represent the values of pixels in images f and g. therefore

$$T: f \longrightarrow g \quad (1)$$

$$s = T(r) \quad (2)$$

T is a 1-1 function that maps f values to g values. If an image is k bit, it can be 2^kgrey level values. Therefore, values can be transform to [0 2^k-1]. Some of useful image enhancements are Contrast Stretching, Logarithmic Transformation, Power-Law Transformations, Piecewise Linear Transformation Functions, Gamma correction, Grey Level Slicing and Histogram Processing[37].

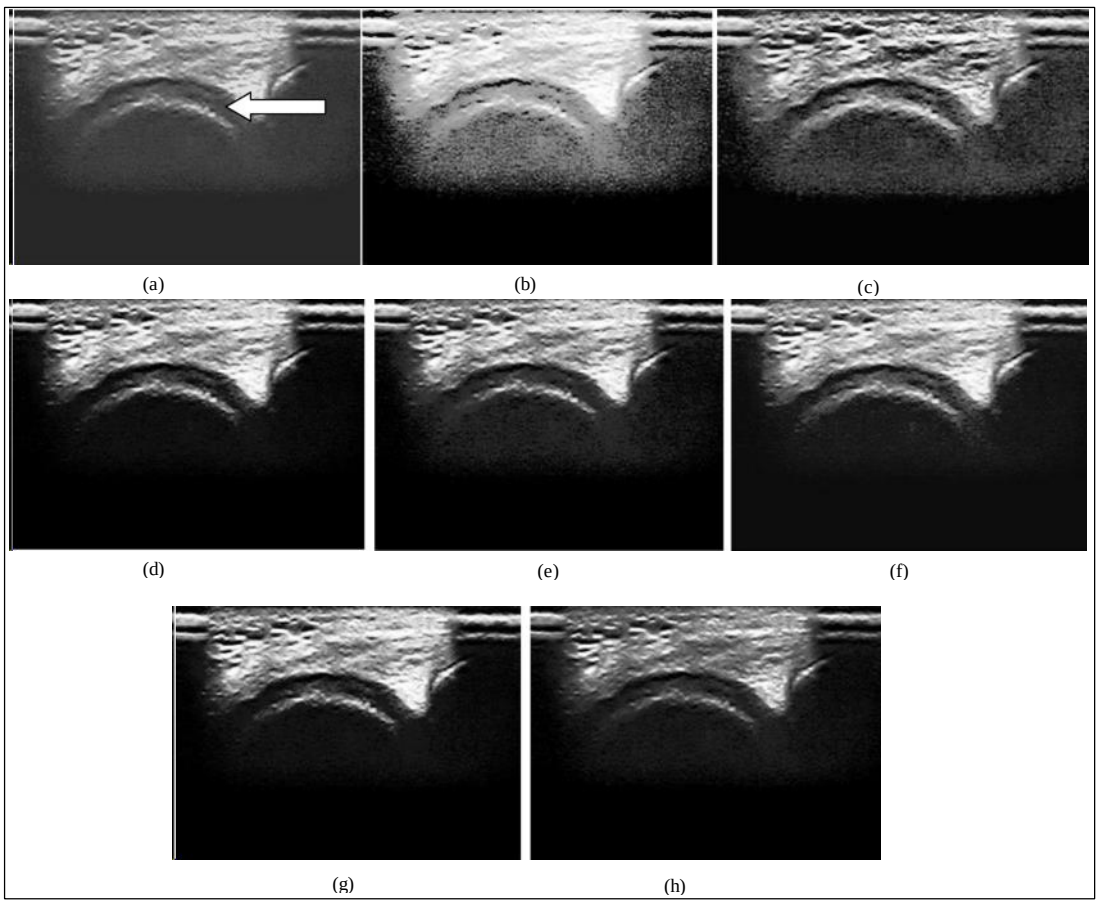

Figure 4: (a)Original cartilage image, (b)conventional, (c)CLAHE, (d)BBH, (e)DSIHE, (f)RSIHE, (g) MMBEBHE (h)MBOBHE (proposed) [38].

In figure 4, an image enhancement technique is implemented for early detection of knee osteoarthritis

2.1.2 Texture Analysis

One of the important properties to identify and recognize images is texture. Nonetheless, there is no formal and complete definition for texture analysis, yet researchers have presented some measurements. The intensity variations in image pixels present texture, which can be seen in nature scene like sand, stones, grass, and leave. Texture presents info regarding the spatial distribution of color or intensity in the image. It refers to the regional intensity variation from one pixel with its neighbors or inside a small region[39]. Texture analysis has played a significant role in medical imaging and it's popular using in this area are segmentation, classification and synthesis. The texture is an significant image characteristic, which has been used to classify same parts and recognize similar objects. Many texture analysis techniques have been represented which could be classified into three basic categories: statistical techniques, statistical techniques, and spectral techniques.

In the statistical technique, some characteristics like smooth, coarse, grainy are calculated. This technique measures texture feature by statistical rules governing the distribution and relation of grey-levels[40]. Some random process is estimated by applying this technique. The commonly used methods in this technique are based on gray level co-occurrence matrix (GLCM). In this method, various textural features are extracted from the image using GLCM [27].Structural technique use images primitive to analysis texture. Structural techniques try to introduce textures using repetitive image primitives [41]. Spectral techniques are based on Fourier functions. Periodic image or almost periodic 2-D Patterns could explain using spectral techniques. The most generally used methods are Fourier spectrum, Bessel-Fourier, Gabor functions and wavelet transform [42].

2.1.3 Co-Occurrence Matrix

Based on gray level co-occurrence, that is the second-order statistics image characteristics are estimated. This matrix is generated consider to the relationship between pixels or two groups of pixels. Gray level co-occurrence has been suggested based on pixels relationship and some primary features were presented based on it and become popular with widely using[43]. Also, many features have been generated based on GLCM with other researchers. GLCM represent the relationship between two intensity pixels at two distinct locations. It calculates the number of times that two intensities locate in the specific position. Figure 5 shows a sample of intensity pixels set and a GLCM based employed for its generation.

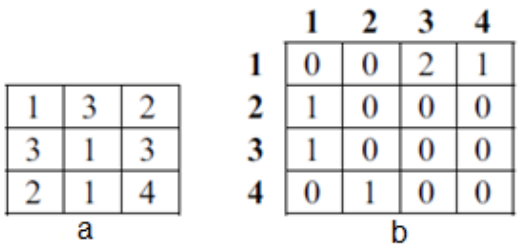

Figure 5: Making GLMC from the original image. a)original image. b)Co-Occurrence matrix[44].

The GLCM is included from P(i,j) which is the probability or the number of occurring i and j along with a given direction and specific at distance. For example, we investigate the relationship between (1,3) in the original image in which the frequency or number of the occurring pixel having gray level 3 is directly connected to the right of the pixel with gray level 1. The number of this condition is equal to the value which is in the (1,3) location of Co-occurrence matrix. The number of rows and columns of Co-occurrence are equal to the number of threshold levels. Because original image has 4 different gray levels intensity, the Co-occurrence matrix is 4 by 4. The distance between neighboring pixels is 1 and can produce different Co-occurrence matrixes in a different direction[45]. In such situation, it's better to select more distant neighbors to generate co-occurrence matrix. Four directions have been presented which are 0, 45, 90, 135 degrees. 14 significant textural descriptors presented based on GLCM to extract texture features[46]. In the following four commonly used descriptors has been presented which is uniformity of energy, contrast, correlation and entropy and defined as

$$Uniformity\ of\ energy = \sum_{i=1}^{n}\sum_{j=1}^{n}\{P(i,j)\}^2 \quad (3)$$

$$Contrast = \sum_{t=1}^{n-1} t^2 \sum_{i=1}^{n}\sum_{j=1}^{n} P(i,j)\ , \qquad t = |i-j| \quad (4)$$

$$Corelation = \frac{1}{\sigma_x\sigma_y}\left[\sum_{i=1}^{n}\sum_{j=1}^{n} i.j.P(i,j) - \mu_x\mu_y\right] \quad (5)$$

$$Energy = -\sum_{i=1}^{n}\sum_{j=1}^{n} P(i,j)\log\{P(i,j)\} \quad (6)$$

3. Segmentation Approaches

In this section, several segmentation techniques employed in recent medical images segmentation are elaborated along with their implementation and pros, cons. Thresholding, region growing, edge based methods which includes region and boundary, are explained in detail. Some learning methods, which include supervised and unsupervised techniques, are also explained. Finally, the latest segmentation approaches such as graph cut, which use both of region, boundary and categorized in the hybrid method are explained at the end of this paper (grab cut- lazy snapping).

3.1. Recent Segmentation Approaches

Lasse et al. [47] introduced a new method for collagen architecture of knee joint. The introduced method is an assessment of the patient outcome for exact collagen architecture in time dependent. This process is captured during the human gait. Kashyap et al. [48] introduced a 4D fully automated method for knee joint segmentation. The introduced method is extended the 3D LOGISMOS method. Satyananda et al. [49] present a learning based knee segmentation method. The introduced method is utilized two random forest classifiers in sequence. The flow chart is shown in figure 5. Prasoon et al. [50] introduced a 2D CNN

method for voxel classification. They have one to one association between 3D images. Tamez et al. [51] introduced an unsupervised method for knee segmentation. It provides precise segmentation, which is further used to extract the surface area, articular cartilage volume, thickness and sub chondral bone plate curvature. Kashyap et al. [52] extend the LOGISMOS method for knee segmentation by maintaining optimality. Wang et al. [53] introduced a multiclass learning technique for segmentation of patellar cartilage, which feats the relative limitations between

cartilage and bone. Zhou et al. [54] perform 3D knee segmentation from three different sequences such as sagittal, coronal and MRI respectively. Mallikarjunaswamy et al. [55] implements a hybrid segmentation method for knee joint segmentation. The region growing method is merged with volume rendering of 3D visualization. Pang et al. [56] introduced an automatic segmentation of cartilage based on three binary classifiers. The binary classifiers are employed by Bayesian theorem for segmentation. Ashan et al. [57] introduced a multi-atlas segmentation technique with patch based label fusion. They assure the spatial and regularity separation of tibial and femoral cartilage. Paproki et al. [58] present an automated segmentation PCL by validating a multi scale patch based method for knee joint segmentation. Gan et al. [59] introduced a random walk based knee joint segmentation. Hong et al. [60] investigate the capability of a random walk for knee joint segmentation. The segmentation is accessed by implementing Dice similarity method. The evaluation is performed on normal cartilage and diseased cartilage. Antony et al. [61] introduced a new method for automatically quantify the severity of knee using X-RAY images. The introduced method is consists of two steps: a) automatically localizing the knee joints; b) classifying the localizing knee joints. Then fully CNN is utilized for accurately detect the knee joints. Swamy et al. [62] improve the problem of knee segmentation using radial search based method and also improve the computation time. Lee et al. [63] present fully automated method for knee joint segmentation using local structural analysis and multi Atlas method. The introduced method efficiently detects the knee joints. Zhang et al. [64] exploit the set of features and spatial dependencies among neighboring voxels. Also, SVM and random field based association and interaction are utilized for classification. Liu et al. [65] segment the knee joints by region based active contour method. Dijia et al. [66] proposed effective and accurate segmentation technique with multiple bones. It uses a model based marginal space learning for pose assessment and flexible border distortion, followed by graph-cut and multi layer graph partition to recover shape details and remove overlapping between bones respectively. Lee et al. [67] segment the knee joints by graph cut method with novel labeled refinement and shape prior.

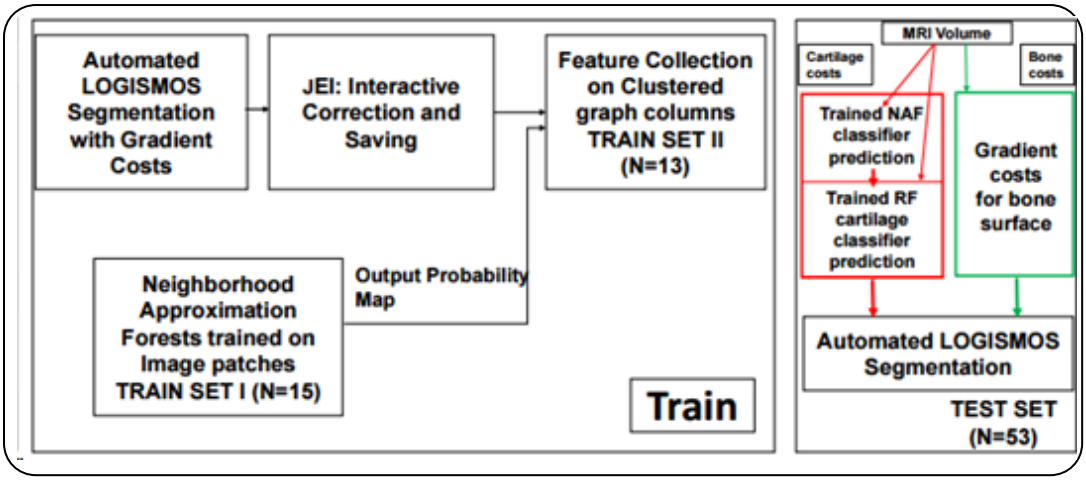

Figure 6: Work Flow of segmentation [49]

Table 1: Description of existing segmentation techniques.

Author	**Year**	**Description**
Lasse et al. [47]	2016	Assessment of the impact of patient-particular collagen design on time subordinate.
Kashyap et al. [48]	2017	A 4D accurate and fully automated segmentation
Kashyap et al. [49]	2016	LOGISMOS algorithm.
Prasoon et al. [50]	2013	Voxel classification integrating three 2D CNN
Tamez et al. [51]	2012	An unsupervised segmentation method, which gives precise segmentation that is further used to extract the surface area, articular cartilage volume, thickness, and subchondral bone plate curvature.
Kashyap et al. [52]	2017	Extended the 4D layered LOGISMOS segmentation method while maintaining optimality.
Wang et al. [53]	2013	A multi class learning technique of segmentation of patellar cartilage, tibial, and femoral is presented.
Zhou et al. [54]	2016	3D
Mallikarjunaswamy et al. [55]	2015	Region growing method along with volume rendering of 3D visualization.
Mahmood et al. [68]	2015	Edge detection and segmentation techniques for knee cartilage visualization.
Pang et al. [56]	2015	An automatic segmentation based on three binary classifiers was built by using Bayesian theorem.
Shan et al. [57]	2014	A multi-atlas segmentation technique with patch based label

		fusion.
Paproki et al. [58]	2016	Presented an automated segmentation PCL by validating a multi scale patch-based technique.
Gan et al. [59]	2017	Presented and analyzed a knee cartilage segmentation method by considering random walks.
Gan et al. [60]	2017	Inter-observer reproducibility
Antony et al. [61]	2017	Automatically detect the knee joints using a fully convolutional neural network (FCN)
Swamy et al. [62]	2013	A semiautomatic method for knee joints segmentation. The radial search method is used search area to reduce computation time

3.1 Region and Boundary Methods

(a) Thresholding

It is simple and fast segmentation method that segment images based on regions with different gray level. The threshold can be defined as the value in the histogram by which intensities of background and foreground pixels can be split into two parts. Pixels with low intensities then threshold value are considered as 'background' on the other hand, Pixels with high or equal values of intensities than the threshold are considered as 'foreground'. Consequently,

$$O(i,j) = \begin{cases} foreground & if\ I(i,j) \geq T \\ Background & if\ I(i,j) < T \end{cases} \quad (7)$$

Where T is the value of threshold, $I(i,j)$ is defined as pixel intensity at location (i,j). Selection of threshold value is dependent on the result of segmentation, if threshold is inappropriate, the result of segmentation would be worse. Multi-thresholding is a type of thresholding in which more than one thresholds are used for separating multiple objects with different grey levels.

In the following images a CT, images of legs has been extracted by performing thresholding segmentation.

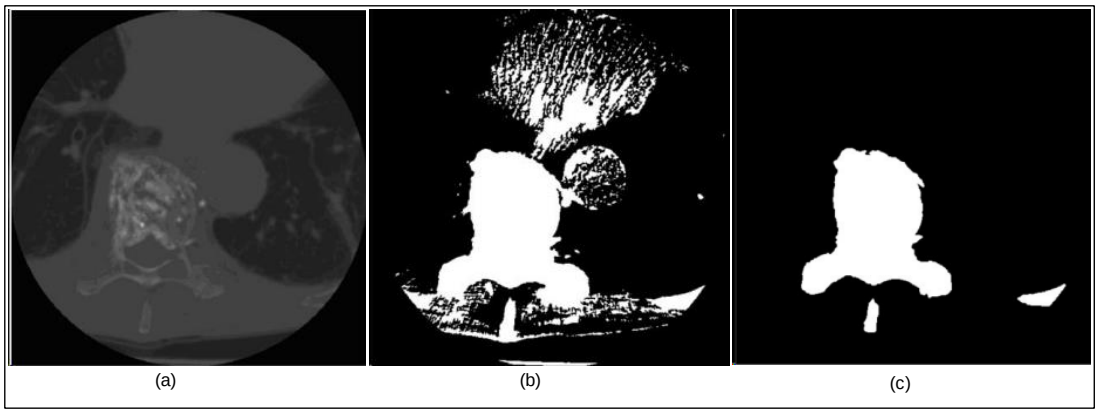

Figure 7: Applying thresholding on CT image: a) original CT images b) initial segmentation. (d) Bone region after iterative adaptive thresholding [45].

(b) Region Growing

Region growing is the collaborative method of segmentation which take the initial seed point for the user and then start the procedure.

Region growing is a collaborative segmentation method, which takes seed point from user as input and then starts the procedure. This method isolates an area of pictures in light of some predefined law as per force data. In the least complex frame, the user should choose one seed point. It will be become in view of its homogeneity properties as per neighbouring pixels [69]. There are a few locales developed based strategies that have a distinction in l rther down, f

Algorithm:

Region_Growing (Input : ς)

- Region $\gamma = \{\varsigma\}$
- While $\gamma.\eta \neq \{\}$

at every value of voxel ν in $\gamma.\eta$, if $g(\nu,\gamma) = true$, then add ν to γ

end while loop

- Return γ

Where ς represents seed, η is neighbour

In above mention algorithm, γ is defined as the region we need to extract. This algorithm shows the basic region growing process which calculates the distance among voxel ν and mean of the region which is delibrated in further down equation:

$$g(v,\gamma)= \left|f(v) - \mu_{\gamma}\right| < \tau \quad (8)$$

Where μ_{γ} is mean of the region 'γ' and 'τ' represents threshold value. Value of threshold can be choosed by automated method or manually. The region growing based segmentation is shown in further down figure.

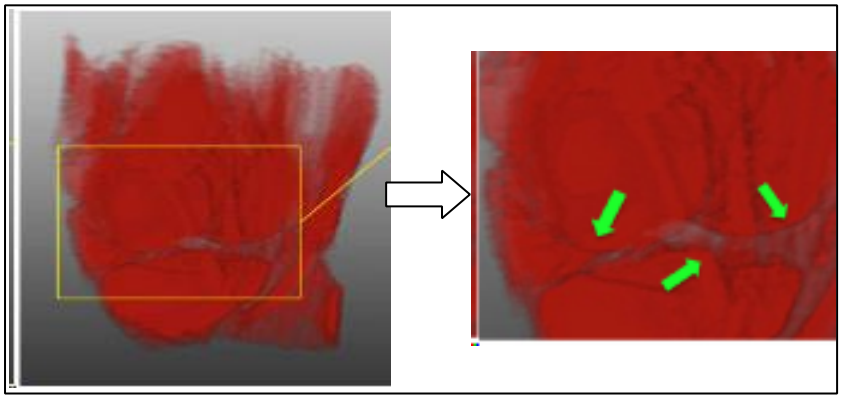

Figure 8: Region growing based segmentation [71].

Table 2: Description of recent segmentation techniques.

Method	**Year**	**Description**
Uozumi et al. [72]	2013	Knee joint segmentation into respective bone via anatomical structure for the knee joint
Lee et al. [63]	2014	A fully automated method for cartilage segmentation by utilizing local structural analysis and multi Atlas method.
Zhang et al. [64]	2013	An automated cartilage segmentation method, which exploits the set of images (magnetic resonance) features and spatial dependencies among neighboring voxels
Liu et al. [65]	2013	Region-based active contour method for knee segmentation.
Dijia et al. [66]	2014	A model based marginal space learning for pose assessment and flexible border distortion, followed by graph-cut and multi layer graph partition method is used
Zhang et al. [73]	2013	A new classification model by using extreme learning machine based association and a discriminative random field based interaction potential.
Lee et al. [67]	2014	A graph cut based segmentation method with novel label refinement and shape prior.

(c) Edge Detection

Edge detection is a boundary based method that is one of the basic tools in image processing and computer vision. Pixels difference rather than pixel similarities is the basic idea of this

method. It can be achieved by following sudden changes in pixels intensity. Edge can be calculated by applying gradient operator on matrix intensity pixels and performing thresholding on the magnitude of gradient image[74].

Most of the clinical work has been done on semi-automatic segmentation. In these techniques, the user needs to select some seed points based on their aims and image characteristics like Region Growing methods, Level Sets, Snakes, Graph Cuts. Some semi-automatic work has been done on meniscus with reasonable accuracy but it is necessary to produce automated method.

(c) Graph Cut approach

An automated segmentation has been done on bone MRI using phase information and applying classification on texture features, although achieving phase information of each MRI slice is not common in imaging and recording MRI data, the results are not bad. Other automated works are applying active shape model on bone-cartilage and performing statistical shape models on bone. The appropriate regions of interest using graph cut based method have shown the best accuracy. During last decade this algorithm has been used widely in image processing and vision applications.

Graph cut is an interactive computer vision method that is the labeling problem and used as segmentation in image processing. The nodes of graph play role as graph's nodes and the edge weight get values from the relationship between pixels. Some pixels are selected as primary foreground and the background area. Some edges are linked this primary area with two extra nodes that called "T" and "S". "T" is related to terminal and used for background area; "S" is related to sink and used for foreground area. A minimum cost cut generates segmentation by producing a cut on graph edges. The whole process is exhibited in Figure 9.

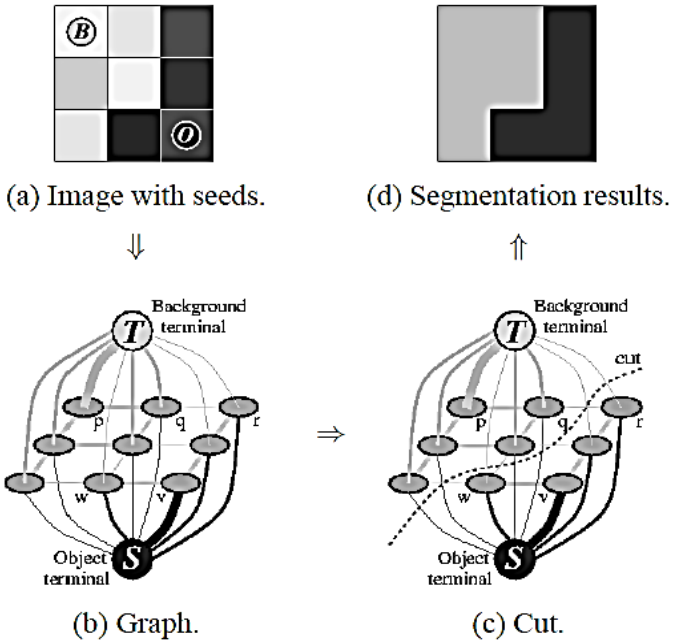

Figure 9: Graph cut: (a) seed points are selected for background and foreground; (b) waited for the graph; (c) calculating Minimum cut; (d) segmentation results. [75]

Graph cut is an interactive segmentation method, means that operator should select some seed point to initialize the algorithm. In recent work, an equation has been produced and has been applied in texture information to produce seed points by block discovery to initialize Graph cut instead of human interactions. The results have been shown in Figure 10.

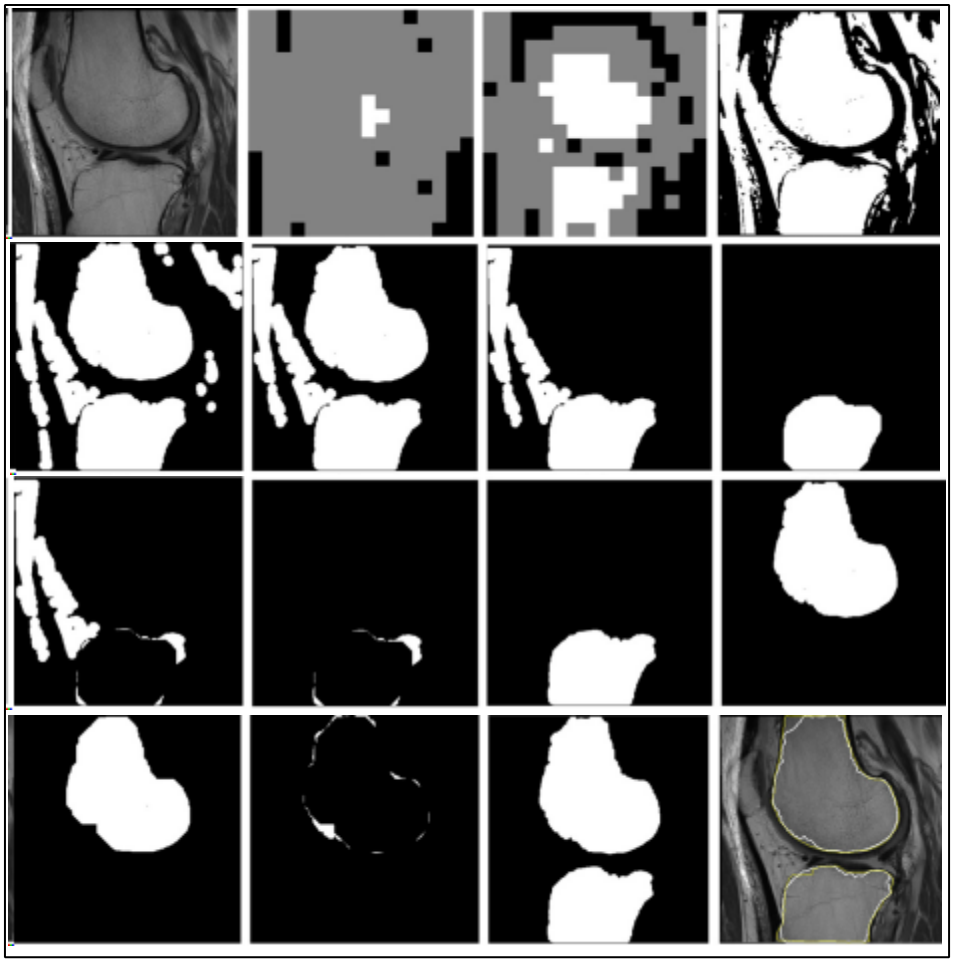

Figure 10: Graph-cut based segmentation results[76].

3.2. Other Approaches

Norouzi et al. [28]applied Graph Cut segmentation method which divides the images into some background parts and an object. The segmentation in this method is performed by applying the minimum cut algorithm, which finds the minimum cut on graph created by the pixels of images. Shan et al.[68]implement the cartilage segmentation by utilizing the three-label segmentation method. Experimental results evaluated that the proposed method shows superior performance 78.2% for femoral cartilage and 82.6% for tibial cartilage. Gan et al. [57]introduced a random walks knee cartilage segmentation model. If compared it with manual segmentation the proposed model has exhibited promising reproducibility in normal and diseased categories. In the literature, Wang et al. [77] applied multiple expert-segmented on images, that is known as atlases. The atlas segmentations are combined using label fusion. Lu et al. [78] applied Scene segmentation method that involves three steps. In step one, segmentation of cell clumps is performed. In step two, nuclei is segmented and detected and then the last step estimates the shape priors and primary cell segmentation for level set method. estimation of the shape priors and introductory divisions of the cells are required for the level set strategy. Dodin et al. [79] developed a completely computerized segmentation

technique for human knee MRI. The proposed strategy depends on Ray Casting technique that depends on disintegration of the MR images into various surface layers. Fujinaga et al. [80] applied semi-automated segmentation software by utilizing an vigorous contour model algorithm to demonstrate calculation of fragmented edge on every cut of 3D picture arrangement. The proposed step provides a more accurate and objective segmentation. Guillemaut et al. [81] proposed a novel method that, under different challenging conditions, can effectively process a good scene depiction by mean of graph-cut optimization of an energy function combining multiple image cues with strong priors. Wang et al. [82] introduced strategy to mutually section an arrangement of pictures containing objects from numerous classes. The proposed method firstly set up reliable useful maps over the info pictures, and present a detailing that unequivocally models fractional likeness over pictures rather than global consistency. Approval with two distinctive datasets is also introduced. Li et al. [83] developed a new region-based technique for segmentation, which can manage intensities in impartialities of segmentation. Swamy et al. [62] introduced a novel method in which knee joint MR images of typical and OA influenced are handled for division and representation of cartilage utilizing self-loader strategy. The spiral pursuit strategy is utilized with minor changes in inquiry zone to diminish calculation period. Cartilage width and bulk is restrained in horizontal, medical and patellar sections of the femur. An SVM classifier is used for classification. Uozumi et al. [72] proposed a new technique that used the anatomical design of knee joint and segments the knee joint into respective bone. In experiments, they calculated the identical rate of manual and the proposed strategy for assessing it. The proposed technique is sufficient to fragment the knee bones [87,88,89].

4. Datasets

4.1.MRI dataset:

The MRI dataset consists 15 normal and 10 diseased Dual Echo Steady state images of 3-Tesla (T). All the images in the dataset have following properties which are used in this experiment: flip angle 25°, section thickness 0.7mm, matrix size 384 × 384, the bandwidth of 185 Hz/pixel, in plane resolution 0.365 ×0.456mm and TR/TE of 16.3/4.7 msec. The presented model is multimodal segmenting characteristics, which allow it to segment the different parts of the knee. Also, the proposed model has a high rate of reproducibility 0.93±0.022 in normal Cartilage and 0.90±0.049 in diseased cartilage as compared to manual segmentation, which has low reproducibility in the both cases of normal cartilage 0.83±0.028 and diseased cartilage 0.79±0.073. That's why the ethnicity of the proposed method is established [84].

4.2.ACL:

The images in the ACL and OA cohort are down sampled to a matrix 5[50350310] iteratively morphed to the space of the reference randomly selected from the dataset. For the morphing, the spline transformation is utilized and further to optimize the figure of the transformation mutual information image similarity matrix is used and this process is repeated, and selected

whole 165 instances in the dataset. At the end, the best reference is selected that is used to minimize the overall dataset [85].

4.3.Co segmentation dataset

For the experiment purpose the proposed technique utilized the two benchmark co segmentation dataset and some downloaded images from the internet. A sample set of the downloaded images is selected and vary β control the overall performance. This dataset holds 30 classes and each class in the dataset have many images. These datasets are evaluated in the previous related work also but the performance this proposed method gave better results [86].

4.4.SKI 10

The ski10 dataset has to 250 Knee MRI originating from the surgical planning program. In the both cases either left or right knee are divided approximately equally. And the data of this dataset is acquired from 80 centers in the USA using Hitachi, Siemens, General Electric and many others. The pixel spacing of the Images is 0.4 0.4 and the distance between the slice is 1mm. the contrast agents are not utilized [57].

4.5.PETUTILE dataset

The UTILE MRI grouping is utilized and obtaining the time of 214 s was accomplished for the head-and-neck region with contrasted and 164 s for a solitary resound UTE examine and 1.75-mm isotropic resolution. The maps of the reciprocal sensitivity show high correlation with the MRI based CT scan and process is same for PET activities. The accuracy is reached to 81.1%. The whole correlation is high and the region of PET activities shows more accurate results in the case of mean and deviation [90-94].

5. Discussion / Conclusion

This paper has presented several techniques for MRI images analysis for knee bone cancer treatment. Accordingly, current methods reported in the state of art are elaborated and their results are compared to benchmark databases. The first group included simple methods like region growing and thresholding. That is followed by classification and clustering methods as the second group of image segmentation. These approaches work on region and boundary using extra information, statistical methods or training sets. The last group includes graph cut method that is based on boundary and region. Most of the works based on semi-automatic methods. However, these methods are sensitive to noise and input values have a profound effect on the accuracy. It is explained earlier that medical images have a noise problem and so this group of methods is not useful. Several researches have been done on the second group, but still, an optimal solution is in demand and so is a hot issue. Nonetheless, they show appropriate results but the best results are belonging to graph cut. Consequently, Graph cut based method has become popular during this decade.

The important benefit of graph cuts is that it calculates a universally optimum segmentation. It could find a general optimum solution for energy functions in the context of image segmentation that could achieve segmentation results with the best accuracy. The results that achieve in recent work in medical images show this method has appropriate performance in this area. It is essential to present instinctive image segmentation technique to analyse and process MRI image specifically knee bone. Many semi-automatic works have been done and providing automatic methods is a challenging work.

As a future prospectus, most important part of this work is to improve traditional graph cut method with a new set of edge weights and using iteration to reduce errors. The second important part of segmentation task is smoothness parameter λ, which has significant effect on segmentation result. Accordingly, we suggest a leaning method to find an appropriate λ value to reduce the effectiveness of this parameter to change the result. Other contribution of this work is finding initial value to seed graph cut method to improve segmentation results.

References

[1] T. Saba, S. Alzorani, and A. Rehman, "Expert system for offline clinical guidelines and treatment," *Life Science Journal*, vol. 9, pp. 2639-2658, 2012.

[2] Abbas, N. Saba, T. Mohamad, D. Rehman, A. Almazyad, A.S. Al-Ghamdi, J.S. (2016) Machine aided malaria parasitemia detection in Giemsa-stained thin blood smears, Neural Computing and Applications, pp. 1-16, doi:10.1007/s00521-016-2474-6,

[3] P. Rahmati, A. Adler, and G. Hamarneh, "Mammography segmentation with maximum likelihood active contours," *Medical image analysis*, vol. 16, pp. 1167-1186, 2012.

[4] S. J. Redmond and C. Heneghan, "A method for initialising the K-means clustering algorithm using kd-trees," *Pattern recognition letters*, vol. 28, pp. 965-973, 2007.

[5] G. Sulong, T. Saba, and A. Rehman, "A new scars removal technique of fingerprint images," in *Instrumentation, Communications, Information Technology, and Biomedical Engineering (ICICI-BME), 2009 International Conference on*, 2009, pp. 131-135.

[6] H. Chen, X. Lei, and D. Yao, "An improved ordered subsets expectation maximization positron emission computerized tomography reconstruction," *Computers in biology and medicine*, vol. 37, pp. 1780-1785, 2007.

[7] Z. Ji, Y. Xia, Q. Chen, Q. Sun, D. Xia, and D. D. Feng, "Fuzzy c-means clustering with weighted image patch for image segmentation," *Applied soft computing*, vol. 12, pp. 1659-1667, 2012.

[8] Z. Muhsin, A. Rehman, A. Altameem, T. Saba, and M. Uddin, "Improved quadtree image segmentation approach to region information," *The Imaging Science Journal*, vol. 62, pp. 56-62, 2014.

[9] M. Mundher, D. Muhamad, A. Rehman, T. Saba, and F. Kausar, "Digital watermarking for images security using discrete slantlet transform," *Applied Mathematics & Information Sciences*, vol. 8, p. 2823, 2014.

[10] K. Neamah, D. Mohamad, T. Saba, and A. Rehman, "Discriminative features mining for offline handwritten signature verification," *3D Research*, vol. 5, p. 2, 2014.

[11] J. Juan-Albarracín, E. Fuster-Garcia, J. V. Manjón, M. Robles, F. Aparici, L. Martí-Bonmatí, *et al.*, "Automated glioblastoma segmentation based on a multiparametric structured unsupervised classification," *PloS one,* vol. 10, p. e0125143, 2015.

[12] A. Rehman, F. Kurniawan, and T. Saba, "An automatic approach for line detection and removal without smash-up characters," *The Imaging Science Journal,* vol. 59, pp. 177-182, 2011.

[13] T. Saba, "Pixel Intensity Based Cumulative Features for Moving Object Tracking (MOT) in Darkness," *3D Research,* vol. 7, pp. 1-6, 2016.

[14] D. Hunter, R. Altman, F. Cicuttini, M. Crema, J. Duryea, F. Eckstein, *et al.*, "OARSI clinical trials recommendations: knee imaging in clinical trials in osteoarthritis," *Osteoarthritis and cartilage,* vol. 23, pp. 698-715, 2015.

[15] A. Lasocki, A. Tsui, M. Tacey, K. Drummond, K. Field, and F. Gaillard, "MRI Grading versus Histology: Predicting Survival of World Health Organization Grade II–IV Astrocytomas," *American Journal of Neuroradiology,* vol. 36, pp. 77-83, 2015.

[16] Y. J. Ryu, S. H. Choi, S. J. Park, T. J. Yun, J.-H. Kim, and C.-H. Sohn, "Glioma: application of whole-tumor texture analysis of diffusion-weighted imaging for the evaluation of tumor heterogeneity," *PLoS One,* vol. 9, p. e108335, 2014.

[17] J. W. J. Lung, M. S. H. Salam, A. Rehman, M. S. M. Rahim, and T. Saba, "Fuzzy phoneme classification using multi-speaker vocal tract length normalization," *IETE Technical Review,* vol. 31, pp. 128-136, 2014.

[18] T. Saba, A. Rehman, and G. Sulong, "An intelligent approach to image denoising," *Journal Of theoretical and Applied information technology,* vol. 17, pp. 32-36, 2010.

[19] A. E. Rad, M. S. M. Rahim, A. Rehman, and T. Saba, "Digital Dental X-ray Database for Caries Screening," *3D Research,* vol. 7, pp. 1-5, 2016.

[20] T. Saba, A. Rehman, and M. Elarbi-Boudihir, "Methods and strategies on off-line cursive touched characters segmentation: a directional review," *Artificial Intelligence Review,* pp. 1-20, 2014.

[21] S. Soleimanizadeh, D. Mohamad, T. Saba, and A. Rehman, "Recognition of partially occluded objects based on the three different color spaces (RGB, YCbCr, HSV)," *3D Research,* vol. 6, pp. 1-10, 2015.

[22] T. Saba and A. Altameem, "Analysis of vision based systems to detect real time goal events in soccer videos," *Applied Artificial Intelligence,* vol. 27, pp. 656-667, 2013.

[23] T. Saba and A. Rehman, "Effects of artificially intelligent tools on pattern recognition," *International Journal of Machine Learning and Cybernetics,* vol. 4, pp. 155-162, 2013.

[24] T. Saba, A. Rehman, A. Al-Dhelaan, and M. Al-Rodhaan, "Evaluation of current documents image denoising techniques: a comparative study," *Applied Artificial Intelligence,* vol. 28, pp. 879-887, 2014.

[25] Z. S. Younus, D. Mohamad, T. Saba, M. H. Alkawaz, A. Rehman, M. Al-Rodhaan, *et al.*, "Content-based image retrieval using PSO and k-means clustering algorithm," *Arabian Journal of Geosciences,* vol. 8, pp. 6211-6224, 2015.

[26] Q. Li, Y. Yan, and H. Wang, "Discriminative Weighted Sparse Partial Least Squares for Human Detection," *IEEE Transactions on Intelligent Transportation Systems,* vol. 17, pp. 1062-1071, 2016.

[27] A. Nodehi, G. Sulong, M. Al-Rodhaan, A. Al-Dhelaan, A. Rehman, and T. Saba, "Intelligent fuzzy approach for fast fractal image compression," *EURASIP Journal on Advances in Signal Processing,* vol. 2014, p. 112, 2014.

[28] M. Harouni, M. Rahim, M. Al-Rodhaan, T. Saba, A. Rehman, and A. Al-Dhelaan, "Online Persian/Arabic script classification without contextual information," *The Imaging Science Journal*, vol. 62, pp. 437-448, 2014.

[29] A. M. Ahmad, G. Sulong, A. Rehman, M. H. Alkawaz, and T. Saba, "Data hiding based on improved exploiting modification direction method and Huffman coding," *Journal of Intelligent Systems*, vol. 23, pp. 451-459, 2014.

[30] A. Norouzi, M. S. M. Rahim, A. Altameem, T. Saba, A. E. Rad, A. Rehman, *et al.*, "Medical image segmentation methods, algorithms, and applications," *IETE Technical Review*, vol. 31, pp. 199-213, 2014.

[31] S. Jadooki, D. Mohamad, T. Saba, A. S. Almazyad, and A. Rehman, "Fused features mining for depth-based hand gesture recognition to classify blind human communication," *Neural Computing and Applications*, pp. 1-10, 2016.

[32] A. Rehman and T. Saba, "Neural networks for document image preprocessing: state of the art," *Artificial Intelligence Review*, vol. 42, pp. 253-273, 2014.

[33] A. Jamal, M. Hazim Alkawaz, A. Rehman, and T. Saba, "Retinal imaging analysis based on vessel detection," *Microscopy Research and Technique*, 2017.

[34] J. Shi, S. Zhou, X. Liu, Q. Zhang, M. Lu, and T. Wang, "Stacked deep polynomial network based representation learning for tumor classification with small ultrasound image dataset," *Neurocomputing*, vol. 194, pp. 87-94, 2016.

[35] A. E. Rad, M. S. Mohd Rahim, A. Rehman, A. Altameem, and T. Saba, "Evaluation of current dental radiographs segmentation approaches in computer-aided applications," *IETE Technical Review*, vol. 30, pp. 210-222, 2013.

[36] Z. Al-Ameen, G. Sulong, A. Rehman, A. Al-Dhelaan, T. Saba, and M. Al-Rodhaan, "An innovative technique for contrast enhancement of computed tomography images using normalized gamma-corrected contrast-limited adaptive histogram equalization," *EURASIP Journal on Advances in Signal Processing*, vol. 2015, p. 32, 2015.

[37] R. Maini and H. Aggarwal, "A comprehensive review of image enhancement techniques," *arXiv preprint arXiv:1003.4053*, 2010.

[38] M. B. Hossain, K. W. Lai, B. Pingguan-Murphy, Y. C. Hum, M. I. M. Salim, and Y. M. Liew, "Contrast enhancement of ultrasound imaging of the knee joint cartilage for early detection of knee osteoarthritis," *Biomedical Signal Processing and Control*, vol. 13, pp. 157-167, 2014.

[39] Z. Zhang, W. V. Stoecker, and R. H. Moss, "Border detection on digitized skin tumor images," *IEEE Transactions on Medical Imaging*, vol. 19, pp. 1128-1143, 2000.

[40] A. Husham, M. Hazim Alkawaz, T. Saba, A. Rehman, and J. Saleh Alghamdi, "Automated nuclei segmentation of malignant using level sets," *Microscopy Research and Technique*, vol. 79, pp. 993-997, 2016.

[41] R. Dalvi, R. Abugharbieh, D. Wilson, and D. R. Wilson, "Multi-contrast MR for enhanced bone imaging and segmentation," in *Engineering in Medicine and Biology Society, 2007. EMBS 2007. 29th Annual International Conference of the IEEE*, 2007, pp. 5620-5623.

[42] M. Swanson, J. Prescott, T. Best, K. Powell, R. Jackson, F. Haq, *et al.*, "Semi-automated segmentation to assess the lateral meniscus in normal and osteoarthritic knees," *Osteoarthritis and cartilage*, vol. 18, pp. 344-353, 2010.

[43] M. S. M. Rahim, A. Norouzi, A. Rehman, and T. Saba, "3D bones segmentation based on CT images visualization," *Biomedical Research*, 2017.

[44] K. Subburaj, D. Kumar, R. B. Souza, H. Alizai, X. Li, T. M. Link, *et al.*, "The acute effect of running on knee articular cartilage and meniscus magnetic resonance

relaxation times in young healthy adults," *The American journal of sports medicine*, p. 0363546512449816, 2012.

[45] J. Zhang, C.-H. Yan, C.-K. Chui, and S.-H. Ong, "Fast segmentation of bone in CT images using 3D adaptive thresholding," *Computers in biology and medicine*, vol. 40, pp. 231-236, 2010.

[46] G. Rabottino, A. Mencattini, M. Salmeri, F. Caselli, and R. Lojacono, "Performance evaluation of a region growing procedure for mammographic breast lesion identification," *Computer Standards & Interfaces*, vol. 33, pp. 128-135, 2011.

[47] L. P. Räsänen, M. E. Mononen, E. Lammentausta, M. T. Nieminen, J. S. Jurvelin, and R. K. Korhonen, "Three dimensional patient-specific collagen architecture modulates cartilage responses in the knee joint during gait," *Computer methods in biomechanics and biomedical engineering*, vol. 19, pp. 1225-1240, 2016.

[48] S. Kashyap, H. Zhang, and M. Sonka, "Accurate Fully Automated 4D Segmentation of Osteoarthritic Knee MRI," *Osteoarthritis and Cartilage*, vol. 25, pp. S227-S228, 2017.

[49] S. Kashyap, I. Oguz, H. Zhang, and M. Sonka, "Automated Segmentation of Knee MRI Using Hierarchical Classifiers and Just Enough Interaction Based Learning: Data from Osteoarthritis Initiative," in *International Conference on Medical Image Computing and Computer-Assisted Intervention*, 2016, pp. 344-351.

[50] A. Prasoon, K. Petersen, C. Igel, F. Lauze, E. Dam, and M. Nielsen, "Deep feature learning for knee cartilage segmentation using a triplanar convolutional neural network," in *International conference on medical image computing and computer-assisted intervention*, 2013, pp. 246-253.

[51] J. G. Tamez-Peña, J. Farber, P. C. Gonzalez, E. Schreyer, E. Schneider, and S. Totterman, "Unsupervised segmentation and quantification of anatomical knee features: data from the Osteoarthritis Initiative," *IEEE Transactions on Biomedical Engineering*, vol. 59, pp. 1177-1186, 2012.

[52] S. Kashyap, H. Zhang, and M. Sonka, "Just Enough Interaction for Fast Minimally Interactive Correction of 4D Segmentation of Knee MRI," *Osteoarthritis and Cartilage*, vol. 25, pp. S224-S225, 2017.

[53] Q. Wang, D. Wu, L. Lu, M. Liu, K. L. Boyer, and S. K. Zhou, "Semantic context forests for learning-based knee cartilage segmentation in 3D MR images," in *International MICCAI Workshop on Medical Computer Vision*, 2013, pp. 105-115.

[54] L. Zhou, R. Chav, T. Cresson, G. Chartrand, and J. de Guise, "3D knee segmentation based on three MRI sequences from different planes," in *Engineering in Medicine and Biology Society (EMBC), 2016 IEEE 38th Annual International Conference of the*, 2016, pp. 1042-1045.

[55] M. Mallikarjunaswamy, M. S. Holi, and R. Raman, "Knee joint menisci segmentation, visualization and quantification using seeded region growing algorithm," *Journal of Medical Imaging and Health Informatics*, vol. 5, pp. 552-560, 2015.

[56] J. Pang, P. Li, M. Qiu, W. Chen, and L. Qiao, "Automatic articular cartilage segmentation based on pattern recognition from knee MRI images," *Journal of digital imaging*, vol. 28, pp. 695-703, 2015.

[57] L. Shan, C. Zach, C. Charles, and M. Niethammer, "Automatic atlas-based three-label cartilage segmentation from MR knee images," *Medical image analysis*, vol. 18, pp. 1233-1246, 2014.

[58] A. Paproki, K. J. Wilson, R. K. Surowiec, C. P. Ho, A. Pant, P. Bourgeat, *et al.*, "Automated segmentation and T2-mapping of the posterior cruciate ligament from

MRI of the knee: Data from the osteoarthritis initiative," in *Biomedical Imaging (ISBI), 2016 IEEE 13th International Symposium on*, 2016, pp. 424-427.

[59] H. S. Gan, K. A. Sayuti, A. H. A. Karim, R. A. M. Rosidi, and A. S. A. Khaizi, "Analysis on Semi-Automated Knee Cartilage Segmentation Model using Inter-Observer Reproducibility: Data from the Osteoarthritis Initiative," in *Proceedings of the 7th International Conference on Bioscience, Biochemistry and Bioinformatics*, 2017, pp. 12-16.

[60] G. Hong-Seng, K. A. Sayuti, and A. H. A. Karim, "Investigation of random walks knee cartilage segmentation model using inter-observer reproducibility: Data from the osteoarthritis initiative," *Bio-Medical Materials and Engineering*, vol. 28, pp. 75-85, 2017.

[61] J. Antony, K. McGuinness, K. Moran, and N. E. O'Connor, "Automatic Detection of Knee Joints and Quantification of Knee Osteoarthritis Severity using Convolutional Neural Networks," *arXiv preprint arXiv:1703.09856*, 2017.

[62] M. M. Swamy and M. S. Holi, "Knee joint articular cartilage segmentation using radial search method, visualization and quantification," *International Journal of Biometrics and Bioinformatics (IJBB)*, vol. 7, p. 1, 2013.

[63] J. G. Lee, S. Gumus, C. H. Moon, C. K. Kwoh, and K. T. Bae, "Fully automated segmentation of cartilage from the MR images of knee using a multi-atlas and local structural analysis method," *Medical physics*, vol. 41, 2014.

[64] K. Zhang, W. Lu, and P. Marziliano, "Automatic knee cartilage segmentation from multi-contrast MR images using support vector machine classification with spatial dependencies," *Magnetic resonance imaging*, vol. 31, pp. 1731-1743, 2013.

[65] L. Liu, Q. Zhang, M. Wu, W. Li, and F. Shang, "Adaptive segmentation of magnetic resonance images with intensity inhomogeneity using level set method," *Magnetic resonance imaging*, vol. 31, pp. 567-574, 2013.

[66] D. Wu, M. Sofka, N. Birkbeck, and S. K. Zhou, "Segmentation of multiple knee bones from CT for orthopedic knee surgery planning," in *International Conference on Medical Image Computing and Computer-Assisted Intervention*, 2014, pp. 372-380.

[67] H. Lee, H. Hong, and J. Kim, "Segmentation of anterior cruciate ligament in knee MR images using graph cuts with patient-specific shape constraints and label refinement," *Computers in biology and medicine*, vol. 55, pp. 1-10, 2014.

[68] N. Mahmood, A. Shah, A. Waqas, A. Abubakar, S. Kamran, and S. B. Zaidi, "Image segmentation methods and edge detection: An application to knee joint articular cartilage edge detection," *Journal of Theoretical and Applied Information Technology*, vol. 71, pp. 87-96, 2015.

[69] S.-b. Hu and P. Shao, "Improved nearest neighbor interpolators based on confidence region in medical image registration," *Biomedical Signal Processing and Control*, vol. 7, pp. 525-536, 2012.

[70] S. Van Cauter, F. De Keyzer, D. M. Sima, A. Croitor Sava, F. D'arco, J. Veraart, *et al.*, "Integrating diffusion kurtosis imaging, dynamic susceptibility-weighted contrast-enhanced MRI, and short echo time chemical shift imaging for grading gliomas," *Neuro-oncology*, vol. 16, pp. 1010-1021, 2014.

[71] A. Aprovitola and L. Gallo, "Knee bone segmentation from MRI: A classification and literature review," *Biocybernetics and Biomedical Engineering*, vol. 36, pp. 437-449, 2016.

[72] Y. Uozumi and K. Nagamune, "An automatic bone segmentation method based on anatomical structure for the knee joint in mdct image," in *Engineering in Medicine*

and Biology Society (EMBC), 2013 35th Annual International Conference of the IEEE, 2013, pp. 7124-7127.

[73] K. Zhang, W. Lu, and P. Marziliano, "The unified extreme learning machines and discriminative random fields for automatic knee cartilage and meniscus segmentation from multi-contrast MR images," *Machine vision and applications*, vol. 24, pp. 1459-1472, 2013.

[74] R. Wang, J. Ma, G. Niu, J. Zheng, Z. Liu, Y. Du, *et al.*, "Differentiation between Solitary Cerebral Metastasis and Astrocytoma on the Basis of Subventricular Zone Involvement on Magnetic Resonance Imaging," *PloS one*, vol. 10, p. e0133480, 2015.

[75] Y. Boykov and G. Funka-Lea, "Graph cuts and efficient ND image segmentation," *International journal of computer vision*, vol. 70, pp. 109-131, 2006.

[76] S. Y. Ababneh, J. W. Prescott, and M. N. Gurcan, "Automatic graph-cut based segmentation of bones from knee magnetic resonance images for osteoarthritis research," *Medical image analysis*, vol. 15, pp. 438-448, 2011.

[77] H. Wang, J. W. Suh, S. R. Das, J. B. Pluta, C. Craige, and P. A. Yushkevich, "Multi-atlas segmentation with joint label fusion," *IEEE transactions on pattern analysis and machine intelligence*, vol. 35, pp. 611-623, 2013.

[78] Z. Lu, G. Carneiro, and A. P. Bradley, "An improved joint optimization of multiple level set functions for the segmentation of overlapping cervical cells," *IEEE Transactions on Image Processing*, vol. 24, pp. 1261-1272, 2015.

[79] P. Dodin, J. Martel-Pelletier, J.-P. Pelletier, and F. Abram, "A fully automated human knee 3D MRI bone segmentation using the ray casting technique," *Medical & biological engineering & computing*, vol. 49, pp. 1413-1424, 2011.

[80] Y. Fujinaga, H. Yoshioka, T. Sakai, Y. Sakai, F. Souza, and P. Lang, "Quantitative measurement of femoral condyle cartilage in the knee by MRI: validation study by multireaders," *Journal of Magnetic Resonance Imaging*, vol. 39, pp. 972-977, 2014.

[81] J.-Y. Guillemaut and A. Hilton, "Joint multi-layer segmentation and reconstruction for free-viewpoint video applications," *International journal of computer vision*, vol. 93, pp. 73-100, 2011.

[82] F. Wang, Q. Huang, M. Ovsjanikov, and L. J. Guibas, "Unsupervised multi-class joint image segmentation," in *Proceedings of the IEEE Conference on Computer Vision and Pattern Recognition*, 2014, pp. 3142-3149.

[83] C. Li, R. Huang, Z. Ding, J. C. Gatenby, D. N. Metaxas, and J. C. Gore, "A level set method for image segmentation in the presence of intensity inhomogeneities with application to MRI," *IEEE Transactions on Image Processing*, vol. 20, pp. 2007-2016, 2011.

[84] J. Pang, J. B. Driban, T. E. McAlindon, J. G. Tamez-Peña, J. Fripp, and E. L. Miller, "On the use of coupled shape priors for segmentation of magnetic resonance images of the knee," *IEEE journal of biomedical and health informatics*, vol. 19, pp. 1153-1167, 2015.

[85] V. Pedoia, X. Li, F. Su, N. Calixto, and S. Majumdar, "Fully automatic analysis of the knee articular cartilage T1ρ relaxation time using voxel-based relaxometry," *Journal of Magnetic Resonance Imaging*, 2015.

[86] M. Rubinstein, A. Joulin, J. Kopf, and C. Liu, "Unsupervised joint object discovery and segmentation in internet images," in *Proceedings of the IEEE conference on computer vision and pattern recognition*, 2013, pp. 1939-1946.

[87] Y. Berker, J. Franke, A. Salomon, M. Palmowski, H. C. Donker, Y. Temur, *et al.*, "MRI-based attenuation correction for hybrid PET/MRI systems: a 4-class tissue

segmentation technique using a combined ultrashort-echo-time/Dixon MRI sequence," *Journal of nuclear medicine*, vol. 53, pp. 796-804, 2012.

[88] Iftikhar, S. Fatima, K. Rehman, A. Almazyad, A.S., Saba, T. (2017) An evolution based hybrid approach for heart diseases classification and associated risk factors identification, Biomedical Research 28 (8), pp. 3451-3455

[89] Rahim, MSM, Norouzi, A. Rehman, A. and Saba, T. (2017) 3D bones segmentation based on CT images visualization, Biomedical Research, vol.28(8), pp.3641-3644

[90] Rahim, MSM, Rehman, A. Kurniawan, F. Saba, T. (2017) Ear biometrics for human classification based on region features mining, Biomedical Research, vol.28 (10), pp.4660-4664

[91] Mughal, B. Muhammad, N. Sharif, M. Saba, T. Rehman, A. (2017) Extraction of breast border and removal of pectoral muscle in wavelet, domain Biomedical Research, vol.28(11), pp. 5041-5043.

[92] Jamal A, Hazim Alkawaz M, Rehman A, Saba T. (2017) Retinal imaging analysis based on vessel detection. Microsc Res Tech. 2017;00:1–13. https://doi.org/10.1002/jemt.

[93] Saba, T. Rehman, A. Altameem, A. Uddin, M. (2014) Annotated comparisons of proposed preprocessing techniques for script recognition, Neural Computing and Applications vol. 25(6), pp. 1337-1347 , doi. 10.1007/s00521-014-1618-9.

[94] Meethongjan,K. Dzulkifli,M. Rehman,A. Altameem,A. Saba, T. (2013) An intelligent fused approach for face recognition, Journal of Intelligent Systems vol.22(2), pp. 197-212.